

# Combining State-Specific Quantum Chemistry and Quantum Monte Carlo for Molecular Excited States

Leon Otis<sup>1</sup> and Eric Neuscamman<sup>2, 3, a)</sup>

<sup>1)</sup>*Department of Physics, University of California Berkeley, CA 94720, USA*

<sup>2)</sup>*Department of Chemistry, University of California Berkeley, CA 94720, USA*

<sup>3)</sup>*Chemical Sciences Division, Lawrence Berkeley National Laboratory, Berkeley, CA, 94720, USA*

(Dated: 16 November 2021)

Through a combination of excited-state-specific quantum chemistry, selected configuration interaction, and variational Monte Carlo, we investigate an approach to predicting vertical excitation energies that achieves high accuracy across a broader range of states than either coupled cluster theory or multi-reference perturbation theory. The approach can be employed in settings beyond the current reach of selected configuration interaction or density matrix renormalization group and retains its high accuracy whether it is treating single excitations, double excitations, or charge transfer excitations. To address the different challenges that arise in these types of states, the method combines excited-state-specific orbital relaxations from complete active space self consistent field theory, an extended active space configuration selection, and improved approaches to optimization and variance-balancing within variational Monte Carlo. In addition to testing in smaller molecules where clear theoretical benchmarks exist, we use the method to offer new benchmark values in triple-zeta-or-better basis sets for a doubly excited state of benzene, a partially-doubly-excited state of uracil, and the widely considered charge transfer state in the tetrafluoroethylene-ethylene system.

## I. INTRODUCTION

The wide variety of different excited states in molecules poses an ongoing challenge for traditional electronic structure methods. Many of the most widely applied and scalable methods may provide satisfactorily accurate predictions for one class of excited states, only to fail on others. When surveying the landscape of electronic structure techniques, this problem of inconsistent performance can be traced to the difficulty of simultaneously satisfying the multiple requirements for accurate treatment of all classes of excited states. First, a method should have the means of correctly describing multiconfigurational character, which is more common among excited states compared to ground states. At the same time, for quantitatively accurate energies, the method must possess an ability to capture weak correlation effects. This effective treatment of strong and weak correlation should be maintained in a balanced fashion for both ground and excited state in order to obtain correct energy differences, and accounting for orbital relaxations may be necessary for cases where orbital shapes differ significantly between the two states. Any potential method with general-purpose applicability to excited states must also satisfy the above considerations in larger molecules and basis sets. After discussing the individual strengths of major quantum chemistry approaches, we present a methodology that satisfies these criteria and exploits wave function sparsity and state-specificity to deliver consistently accurate excitation energies across a wide range of molecules and types of excited states.

Time-dependent density functional theory (TDDFT) is by far the most commonly used approach for excited states and has played a leading role in the modeling of absorption

spectra.<sup>1</sup> However, TDDFT has historically struggled, at least for its most common functional choices within the adiabatic approximation, to describe some classes of excited states accurately, with double excitations and charge transfer (CT) as two notorious examples.<sup>2–5</sup> While TDDFT continues to benefit from extensive research<sup>6–9</sup> analyzing and improving approximate functionals, these categories of excited states remain challenging and the ever-growing array<sup>10,11</sup> of possible functional choices motivates the development and use of methods with greater predictive power in these areas.

Among wave function approaches to excited states, coupled cluster theory is a natural initial option to consider, given its prowess for ground state properties and its effective treatment of weak correlation.<sup>12–14</sup> Excited state extensions of coupled cluster, particularly the equation-of-motion formulation,<sup>15</sup> have become widely used at different levels of cluster truncation. For single valence excitations, limiting the excitation level to singles and doubles with EOM-CCSD obtains balanced results with a systematic error of only a few tenths of an eV.<sup>16</sup> Higher orders can achieve even better accuracy.<sup>17</sup> However, for double excitations, EOM-CCSD produces substantially larger errors than for single excitations<sup>18</sup> and while higher orders of coupled cluster can obtain accurate results in some cases,<sup>19</sup> their errors can still be as large as half an eV or worse for pure double excitations.<sup>20</sup> Besides these inaccuracies, the high scalings of coupled cluster methods,  $O(N^8)$  and  $O(N^{10})$  for EOM-CCSDT and EOM-CCSDTQ respectively, hinders their application to larger molecules, even for favorable categories of excited states.

Coupled cluster's difficulties have helped motivate widespread use of multireference approaches such as CASPT2 to address doubly excited states.<sup>20–32</sup> While CASPT2 faces its own limitations due to intruder states, sensitivity to active space and state-averaging choices, and the limiting of dynamic correlation treatment to the PT2 level, it is still capable of obtaining accurate excitation energies,

<sup>a)</sup>Electronic mail: eneuscamman@berkeley.edu

most notably for the pure double excitations where coupled cluster struggles the most.<sup>20</sup> However, for CT states, the situation is reversed, with the use of state-averaging<sup>33</sup> biasing the CASPT2 orbitals to the ground state and producing significant errors.<sup>34–36</sup> In contrast, recent efforts to build accurate benchmark sets for CT states, which are currently less common than for other classes of excited states, have relied upon coupled cluster.<sup>37–39</sup> This problem of inconsistent performance across the diverse array of possible excited states makes the development of more broadly reliable tools a key priority in electronic structure.

While a number of methods,<sup>40,41</sup> including selected CI (sCI),<sup>17,20,42–44</sup> density matrix renormalization group (DMRG),<sup>45,46</sup> and full configuration interaction quantum Monte Carlo (FCIQMC),<sup>47–51</sup> can achieve this reliability with systematic exploitation of wave function sparsity and/or compressibility, their high scaling limits their prospects for extensions beyond small systems. A recent study<sup>40</sup> of benzene is a useful demonstration of the state-of-art capabilities of this collection of high accuracy techniques. The determination of benzene's ground state energy in a double- $\zeta$  basis set is both an important example of the molecular sizes that these high-level approaches can now treat and a reminder of the challenges they face in larger systems and the larger basis sets needed for excited state accuracy. So far, the role of sCI, DMRG, and FCIQMC in larger molecules beyond benzene has been limited to mostly serving as (impressively large) active space solvers.<sup>52–56</sup> Thus, whether one looks to coupled cluster, multi-reference perturbation theory, or the modern array of sparsity and compressibility approaches, it remains challenging to deliver consistently accurate excitation energies in larger molecules, larger basis sets, and across widely differing classes of excitations.

In pursuit of this challenge, we adopt an approach that combines the advantages of excited-state-specific quantum chemistry, sCI, and variational Monte Carlo (VMC). The combination<sup>57–63</sup> of sCI and QMC can be especially effective thanks to the determinant expansions' leveraging of wave function sparsity and the efficacy of Jastrow factors<sup>64–76</sup> for addressing weak correlation effects that sCI is less efficient for. While excited state VMC approaches in this area that use state-averaging are highly effective in many systems,<sup>62,77–82</sup> we choose to employ state-specific formulations of VMC<sup>64,83,84</sup> in order to avoid the same challenges that state-averaged CASPT2 faces in charge transfer states. Further, although recent advances in VMC orbital optimization<sup>85,86</sup> can be employed for state-specific optimization,<sup>87,88</sup> our experience has been that orbital optimization significantly increases the difficulty and cost of the overall VMC ansatz optimization when compared to optimizing CI coefficients and Jastrow parameters alone. In the present study, we therefore hypothesize that orbitals taken from excited-state-specific complete active space self-consistent field theory (SS-CASSCF)<sup>36,89,90</sup> will be sufficiently close to optimal that accurate excitation energy predictions can be made without further optimization within VMC. With these quantum-chemistry-derived excited state orbitals, we employ sCI in an extended active space to identify the elec-

tron configurations that are most helpful in treating the strong and the leading weak correlation effects. This qualitatively correct but not quantitatively accurate wave function is then fed into excited-state-specific VMC, where the configuration interaction expansion is re-optimized alongside explicit (Jastrow) correlation factors. Finally, as these wave functions are still not exhaustively accurate in larger molecules and basis sets, we use VMC to balance the accuracy of the ground and excited state approximations through variance matching<sup>87,88,91,92</sup> in an attempt to explicitly enforce error cancellation in the energy differences between ground and excited states.

This combination of quantum chemistry with VMC offers a number of key advantages. The explicitly multi-reference character is essential when treating difficult double excitations and in states with significant mixtures of singly and doubly excited character. By avoiding state averaging, charge transfer states are provided with fully appropriate post-excitation orbital relaxations and, in the results below, we find that stopping the orbital optimization after the SS-CASSCF stage is sufficient for high accuracy. For weak correlation effects, the use of Jastrow factors and a modest but sCI-chosen configuration interaction expansion appears to be sufficient for the error cancellation balance of variance matching to do its job and deliver 0.1 eV accuracies in all systems tested in which a reliable theoretical benchmark exists. This interplay between variance matching, Jastrow factors, and the limited CI expansion is crucial, as it allows us to push into larger molecules and basis sets than can be reached by approaches that rely on sCI alone and thus require much more exhaustive CI expansions. Finally, it is important to point out that the approximations employed in this approach are quite different than those used in EOM-CC, which allows us to validate coupled cluster results in some circumstances where it is not otherwise obvious (e.g. due to partial doubly excited character) how accurate coupled cluster should be. When these methods agree about a challenging excitation energy, such as in the  $3^1A'$  state of uracil or the tetrafluoroethylene-ethylene charge transfer, the fact that they rely on very different assumptions and approximations increases our confidence in the accuracy of the prediction. We therefore hope that, in addition to its long-standing role in providing ground state reference data in both molecular<sup>93</sup> and solid-state<sup>94</sup> settings, quantum Monte Carlo can, in tandem with excited-state-specific quantum chemistry and coupled cluster theory, be increasingly helpful in this regard in challenging molecular excited states.

To make this combined approach as practical as possible, we have also explored technical improvements to the VMC optimization and variance matching algorithms. Methods for optimizing wave functions in VMC have improved steadily in recent years,<sup>95–100</sup> with variants of the linear method (LM) and accelerated descent (AD) showing particular progress. Building on our recent work on a hybrid optimization approach that combines a blocked variant<sup>98</sup> of the LM with AD,<sup>92,101</sup> we adopt a simple scheme for deciding which parameters are most likely to benefit from the LM optimization step and which can be left for AD to optimized. We also deploy a more practical variance matching approach that in most

cases allows us to avoid building multiple CI expansions for interpolation purposes and thus simplifies calculations in most cases.

We investigate the effectiveness of the overall approach and these technical improvements by surveying a range of different types of excited states. By drawing upon recent benchmark sets<sup>17,20</sup> and our own quantum chemistry calculations, we are able to demonstrate the efficacy of our SS-CASSCF/sCI/VMC approach in single, double, and charge transfer excited states, reaching 0.1 eV accuracy in all cases where rigorous benchmarks are available. In some larger systems, where such benchmarks are not available, we are still able to establish close agreement between our approach and the highest-affordable levels of coupled cluster theory. In a challenging doubly-excited state of benzene where coupled cluster is simply not appropriate, we are able to offer some clarity amidst the range of predictions made by different variants of CASPT2. Taken together, the results indicate that the combination of state-specific quantum chemistry, sCI, and VMC can offer new clarity for excited states in a wide range of molecules that are either too difficult or too large for other high-accuracy electronic structure methods.

## II. THEORY

### A. Excited State-Specific Variational Monte Carlo

The application of VMC to excited states is an active area of method development with multiple possible approaches, including the examples of both state-averaged energy minimization<sup>62,77–82</sup> and state-specific variance-based minimization shown below.<sup>64,83,84,87,88,92</sup>

$$\Omega(\Psi) = \frac{\langle \Psi | (\omega - H) | \Psi \rangle}{\langle \Psi | (\omega - H)^2 | \Psi \rangle} \quad (1)$$

$$W(\Psi) = \langle \Psi | (\omega - H)^2 | \Psi \rangle \quad (2)$$

$$E^{SA} = \sum_I w_I \frac{\langle \Psi^I | H | \Psi^I \rangle}{\langle \Psi^I | \Psi^I \rangle} \quad (3)$$

We employ the state-specific objective function<sup>83</sup>  $\Omega$ , which targets the lowest state above  $\omega$  in energy when minimized. To achieve size-consistent results, the input  $\omega$  must be updated to  $E - \sigma$ , the difference between the energy and the standard deviation, which transforms the optimization of  $\Omega$  into state-specific variance minimization.<sup>84</sup> There are multiple approaches to varying  $\omega$ , but in this work we simply conduct multiple fixed- $\omega$  calculations and change the value of  $\omega$  between each one until self-consistency between it and  $E - \sigma$  is reached. In practice, only a few such fixed- $\omega$  optimizations are needed for any one state.

In contrast to the deterministic methods that are predominantly used in electronic structure, QMC must obtain stochastic estimates of the energy and all related quantities, and practitioners have flexibility in choosing probability distributions for performing efficient Monte Carlo integration. While the distribution  $\rho(\mathbf{R}) = \frac{\Psi(\mathbf{R})^2}{\int d\mathbf{R}\Psi(\mathbf{R})^2}$  is a common choice and has a zero variance property<sup>102</sup> when  $\Psi$  is an exact eigenstate, it suffers from an infinite variance problem with approximate  $\Psi$  in the estimation of other key quantities, particularly the variance and wave function derivatives. To address this issue, regularization schemes,<sup>103,104</sup> estimator modifications,<sup>102,105,106</sup> and other importance sampling functions<sup>87,91,92,107–109</sup> have all been variously employed by the QMC community. We use the same importance sampling function

$$|\Phi|^2 = |\Psi|^2 + c_1 \sum_i |\Psi^i|^2 + c_2 \sum_j |\Psi^j|^2 + c_3 \sum_k |\Psi^k|^2 \quad (4)$$

that was previously used and more fully discussed in recent work.<sup>92</sup> The coefficients  $c_1, c_2, c_3$  weight the sums of squares of wave function parameter derivatives, divided between Jastrow, CI, and orbital parameters respectively. We have found that setting  $(c_1, c_2, c_3) = (0.0, 0.0001, 0.0)$  is a reasonably effective choice for the molecules we consider.

### B. Hybrid Optimization

The stochastic nature of QMC increases the difficulty of its wave function ansatz optimization compared to the analogous problem encountered in deterministic methods. Optimization has been a long-running challenge in QMC method development for many years with a variety of algorithms being introduced. These include the linear method<sup>95,110–112</sup> and accelerated descent<sup>99–101,113,114</sup> approaches. Neither of these classes of methods is fully satisfactory, with the LM possessing a tendency for poor parameter updates due to stochastic step uncertainty with large numbers of variables and AD suffering from slow convergence to optimal parameter values.

We have recently developed a hybrid combination of the blocked version of the LM<sup>98</sup> with AD, first for ground state energy minimization<sup>101</sup> and then for variance-based excited state optimization.<sup>92</sup> In this approach, alternating between sections of descent optimization and the blocked LM enables more efficient convergence to the minimum than using either method on its own. The blocked LM is able to move parameters to the vicinity of the minimum more swiftly than descent, but descent is able to correct for any poor parameter updates made by the blocked LM due to step uncertainty, which makes it useful for converging more tightly. Throughout all our optimizations, we alternate between 100 iterations of AD and 3 steps of blocked LM and refer to one set of both as a macro-iteration. A typical optimization consists of a small number of macro-iterations followed by 1100 iterations of AD with final energy, target function, and variance averages taken over the final 500 iterations. Details on the numbers of macro-iterations and sampling effort used can be found in Appendix

B. These averages and the excited state optimizations are then used in our variance matching procedure, discussed below, to obtain a final excitation energy result. More extensive discussions of our hybrid method can be found in earlier papers<sup>92,101</sup> and in this benchmarking study, we use the same combination of Nesterov momentum with RMSprop and the same hyper-parameter choices as before.<sup>92</sup>

One new element of our optimization approach is to filter the parameters updated by the blocked LM according to the statistical significance of the target function's parameter derivatives, an approach has been successfully used in the past by the QMC community.<sup>115</sup> We use the criterion:

$$\left| \frac{\langle \frac{\partial \Omega}{\partial p} \rangle}{\sigma_{\frac{\partial \Omega}{\partial p}}} \right| > 1 \quad (5)$$

The mean value of the parameter derivative must be at least as large as the standard deviation of that derivative estimate in order for the parameter to be included for the blocked LM update on that iteration. The number and identity of the parameters that are turned off by this filtration stage will vary from LM step to LM step in practice, but we have found that filtering out roughly a third of the parameter set on each blocked LM iteration is a typical occurrence in our optimizations.

We also note that the filtered parameter space is further reduced by the blocked LM algorithm,<sup>98</sup> which divides the parameter set into blocks for LM-style diagonalizations. A limited number of eigenvectors are retained from each block to form the space for a second diagonalization that determines the final parameter update. In our optimizations, we have found dividing the remaining parameters into 5 blocks and retaining 30 parameter directions per block for the second stage of the blocked LM to be an effective choice. The use of the initial filtration stage allows for an automated identification of a smaller variable space that the blocked LM can treat with reduced step uncertainty. The AD sections of the hybrid method continue to optimize all the variational parameters. This refinement of the hybrid method enhances the effectiveness of the blocked LM on moving the most important parameters while allowing AD to handle the remaining parameter adjustments.

### C. Wave Functions

The wave function ansatzes we use in our VMC optimizations are constructed from a preceding set of quantum chemistry calculations. In particular, we obtain molecular orbitals from a recently developed SS-CASSCF,<sup>36,89</sup> which uses a density matrix-based variational principle to track individual states during CASSCF's CI and orbital relaxation optimization steps. When successfully converged, SS-CASSCF can avoid root-flipping and obtain orbitals tailored specifically for the targeted state. We then employ sCI, specifically heatbath CI,<sup>116,117</sup> to generate a set of the most important determinants for a state from a larger active space of our state-specific orbitals. We emphasize that converging the sCI is unnecessary and that in practice we often need only the first few hundred to

few thousand most important determinants for effective initial wave functions within VMC. With the addition of one- and two-body Jastrow factors, we arrive at the form of the multi-Slater Jastrow (MSJ) ansatz that we use for all the molecules we consider in this work.

$$\Psi = \psi_{MS} \psi_J \quad (6)$$

$$\psi_{MS} = \sum_{i=0}^{N_D} c_i D_i \quad (7)$$

$$\psi_J = \exp \left\{ \sum_i \sum_j \chi_k (|r_i - R_j|) + \sum_k \sum_{l>k} u_{kl} (|r_k - r_l|) \right\} \quad (8)$$

We construct the Jastrow factor  $\psi_J$  with splines for the functions  $\chi_k$  and  $u_{kl}$ .<sup>118</sup> As we will show in our results, only limited numbers of the determinants  $D_i$  are needed to obtain highly accurate excitation energies in many molecules.

In all our VMC results, only the Jastrow factors and the determinant coefficients  $c_i$  are optimized by our hybrid method, while the orbitals are left at their SS-CASSCF shapes. While recent developments<sup>85,86</sup> with the table method have made orbital optimization at the VMC level more efficient, it remains more computationally demanding than the Jastrow and CI optimization, and significantly increases the difficulty of our optimization problem. Our decision to use SS-CASSCF orbital shapes and avoid any VMC orbital optimization enables us to obtain significant computational savings while retaining the benefits of state-specificity, particularly in cases with important orbital relaxation effects such as charge transfer. As our results show, leaving the orbitals at their SS-CASSCF shapes does not prevent us from obtaining accurate results, suggesting that the lion's share of orbital relaxation is present already in the active space picture.

### D. Variance Matching

Another key part of obtaining a high level of accuracy with compact wave functions is ensuring a balanced treatment of both ground and excited state in order to benefit from cancellation of errors. Past work has shown that matching the variance between ground and excited state improves excitation energy predictions, but these studies<sup>87,88,91,92</sup> employed various different protocols for obtaining a match and often required additional VMC optimizations at a variety of Slater determinant expansion lengths.

In this work, we introduce a simplified variance matching procedure that reduces the need for considering different numbers of determinants. Once we have a given ground state optimization with some number of determinants and a final variance, we perform an excited state optimization for some chosen CI expansion length. We plot the energies and variances obtained on the blocked LM iterations of this optimization, leaving aside those from the first macro-iteration when

the wave function is still mostly unoptimized. A linear fit to these points provides us with a correction to the excited state energy once its variance has been extrapolated to match the ground state variance, and all the excitation energies we report were obtained from this protocol. Figure 1 and Table I provide an example of the procedure in the case of ketene.

The uncertainty in the excitation energy due to the extrapolation can be estimated from the effect of the stochastic uncertainties in the positions of the energy-variance points on the regression slope. The individual uncertainties in the points can define normal distributions for generating sets of slightly shifted points with their own regression slopes and corresponding excitation energy results. We can then determine an uncertainty in our excitation energy prediction from the uncertainty in the slope used in the extrapolation. In the limits of either an explicit variance match between ground and excited state or a deterministic optimization from infinite sampling, this extrapolation uncertainty will go to zero. Table XIX in Appendix B provides values for this extrapolation uncertainty for all the systems we consider. All excitation energy uncertainties we report in the main text are the sum of the uncertainty from stochastic averaging and the extrapolation uncertainty.

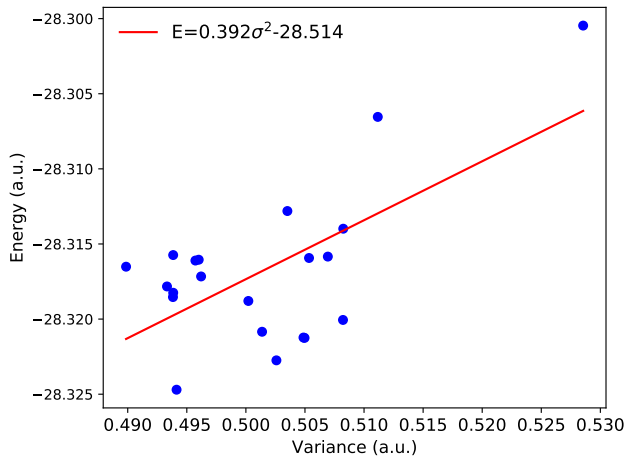


FIG. 1. Example of the linear regression used in variance matching. The points are energies and variances from individual blocked LM iterations in the optimization of the excited state of ketene. See Table I for how the variance matching affects the excitation energy prediction.

TABLE I. Energy and variance values in ketene before and after the variance matching procedure. As shown later in Table II, the final excitation energy prediction is very accurate compared to the literature theoretical best estimate of 3.86 eV.<sup>17</sup>

	Energy (a.u.)	Variance (a.u.)	Excitation Energy (eV)
GS	-28.4813	0.456	
ES Before Match	-28.3226	0.494	4.32
ES After Match	-28.3375	0.456	3.91

This approach reduces the need to perform further opti-

mizations with other numbers of determinants, a requirement when searching for an explicit variance match<sup>92</sup> or for performing an interpolation,<sup>88</sup> making the present methodology easier to apply. The respective numbers of determinants used for the ground and excited state optimizations are chosen based on experience, but can be systematically increased if necessary. In general, longer expansions will be needed to maintain the same level of accuracy in larger systems, and the results we have obtained after systematically increasing from smaller expansions may provide some guidance when considering other molecules of similar sizes.

### III. RESULTS

#### A. Computational Protocol and Technical Details

All our VMC calculations used a development version of QMCPACK.<sup>118,119</sup> In all cases, we used the pseudopotentials and associated basis sets developed by Mitas and coworkers.<sup>120</sup> Molecular geometries were taken from literature benchmark sets<sup>17,20,26,38</sup> and coordinates are also listed in Appendix A. State-specific molecular orbitals were generated by an implementation of SS-CASSCF<sup>36,89</sup> in a development version of PySCF.<sup>121</sup> We generated sCI expansions in expanded active spaces with Dice,<sup>116,117</sup> iterating until at least a million determinants had been selected and then taking those with the largest coefficients into our VMC wave function. The particular active space and basis set choices for different molecules are given in the following sections for each set of excited states. For the charge transfer states we study, we have performed coupled cluster calculations in Molpro<sup>122</sup> and GAMESS<sup>123</sup> for comparisons against our VMC results.

Once our ansatzes were generated, the CI coefficients were optimized within VMC simultaneously with one- and two-body Jastrow factors. The Jastrow factor splines each consisted of 10 coefficients defining the function within a distance of 10 bohr. With two exceptions, the initial value of the Jastrow coefficients was set to zero in all cases and CI coefficients were begun at their values from sCI. In the case of nitrosomethane, the final 1000 determinant excited state optimization began from the result of a previous optimization of the Jastrow and 500 determinants, with the next 500 most important determinants from sCI added with initial coefficients of zero. For the excited state of tetrafluoroethylene-ethylene, the optimized values of the ground state Jastrow were used for the excited state initial guess alongside the sCI coefficients. Further technical details on optimization procedure and the uncertainties in our excitation energies can be found in Appendix B.

#### B. Valence Single Excitations: Thioformaldehyde, Methanimine, and Ketene

In testing our methodology, we begin by considering valence single excitations, specifically the  ${}^1A_2(n \rightarrow \pi^*)$  excited

state in thioformaldehyde, the  ${}^1A''(n \rightarrow \pi^*)$  state in methanimine, and the  ${}^1A_2(\pi \rightarrow \pi^*)$  state in ketene. For these three excited states, sCI and high level coupled cluster results<sup>17</sup> from Loos and coworkers are reliable references for assessing the accuracy of our approach. We generated our SS-CASSCF orbitals using a (12e,10o) active space for thioformaldehyde, a (12e,12o) space for methanimine and a (8e,8o) space for ketene, with pseudopotentials and cc-pVTZ basis sets for all molecules.<sup>120</sup> The subsequent sCI calculations in Dice<sup>116,117</sup> correlated 12 electrons in 17 orbitals for thioformaldehyde, 12 electrons in 18 orbitals for methanimine, and 16 electrons in 22 orbitals for ketene.

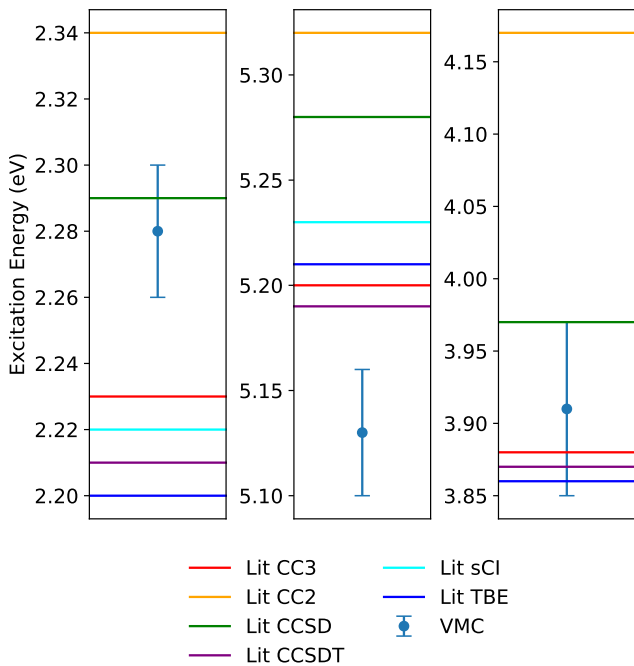


FIG. 2. From left to right, excitation energies in thioformaldehyde, methanimine, and ketene for VMC and quantum chemistry approaches. See also Table II. Reference values for coupled cluster, and selected CI are taken from the work of Loos and coworkers.<sup>17</sup>

TABLE II. Excitation energies for thioformaldehyde, methanimine, and ketene. The VMC uncertainties on the final digits are given in parentheses. The included literature values use an aug-cc-pVTZ basis set for sCI and coupled cluster, and the literature TBEs are obtained from applying a basis set correction using CC3 to the sCI result.<sup>17</sup>

Method	Thioformaldehyde	Methanimine	Ketene
VMC	2.28(2)	5.13(3)	3.91(6)
CC2	2.34	5.32	4.17
CCSD	2.29	5.28	3.97
CC3	2.23	5.20	3.88
CCSDT	2.21	5.19	3.87
sCI	2.22	5.23	3.86
Lit TBE	2.20	5.21	3.86

Our results for this trio of small molecules, depicted visually in Figure 2 with precise values in Table II, show that

our VMC methodology is highly accurate. In all cases, our final excitation energies are within 0.1 eV of the theoretical best estimates determined by Loos and coworkers from basis set corrected sCI calculations. We also emphasize that our results require only relatively simple wave function ansatzes. We used 700 determinants for the ground state and 300 for the excited state in thioformaldehyde, 300 ground and 500 excited for methanimine, and 500 ground and 700 excited for ketene. Thioformaldehyde was somewhat unusual with the ground state having the higher variance for fewer determinants so a longer expansion was optimized for a better variance match with the excited state. The VMC wave functions used in these systems are significantly less complex than those obtainable by coupled cluster and the absolute energies from VMC are comparable to those of CCSD. The excitation energy differences from VMC are also most comparable to CCSD in terms of accuracy, as CC3 and CCSDT are within one or two hundredths of an eV of the sCI-based TBEs. While VMC does not obtain the exquisite accuracy of higher level coupled cluster in these cases, these results are a reassuring check that our approach agrees with very well established quantum chemistry treatments of this generally easier class of excited states, and we now turn our attention to more challenging categories.

### C. Double Excitations: Carbon Trimer, Nitrosomethane, Hexatriene, and Benzene

We next address double excitations, which are a far more challenging class of excited states for coupled cluster. Past work<sup>92</sup> applying VMC to double excitations showed a high level of accuracy and we again draw from the wealth of benchmarking data<sup>20</sup> from Loos and coworkers, comparing our refined SS-CASSCF/VMC methodology to their quantum chemistry values in four molecules. We first consider two small systems, the carbon trimer and nitrosomethane, where highly reliable excitation energies can still be established by sCI, before studying hexatriene and benzene, which are considerably larger cases where less definitive methods must be used. For our ansatz construction, SS-CASSCF orbitals were obtained from a (12e,12o) space for the carbon trimer, a (12e,9o) space for nitrosomethane, and (6e,6o) spaces for hexatriene and benzene. At the sCI stage, these spaces were expanded to (12e,18o), (18e,22o), (32e,46o), and (30e,46o) respectively. For all four molecules, we have used cc-pVTZ basis sets and pseudopotentials.<sup>120</sup>

Concentrating first on the two smaller systems, we see in Figure 3 and Table III that our VMC approach is again highly accurate and within 0.1 eV of the TBEs obtained from sCI. Both states can be classified as pure double excitations based on the low percentage of  $T_1$  amplitudes in CC3<sup>20</sup> and we see that CC3 makes substantial errors of an eV or worse for this type of doubly excited state. Shouldering the expense of full triples with CCSDT only manages to eliminate about half of CC3's errors. In contrast, CASPT2's multireference nature makes it far more successful in this situation and it achieves comparable accuracy to our VMC results in both molecules.

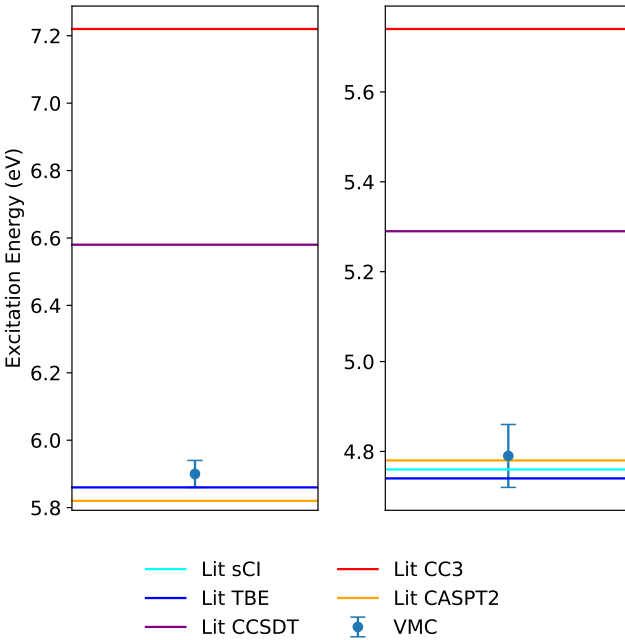


FIG. 3. Excitation energies in the carbon trimer and nitrosomethane in the left and right panels respectively. See also Table III. For the carbon trimer, VMC used 100 determinants in the ground state and 500 for the excited state, while 500 and 1000 respectively were used for nitrosomethane. Reference values for coupled cluster, and selected CI are taken from the work of Loos and coworkers.<sup>20</sup>

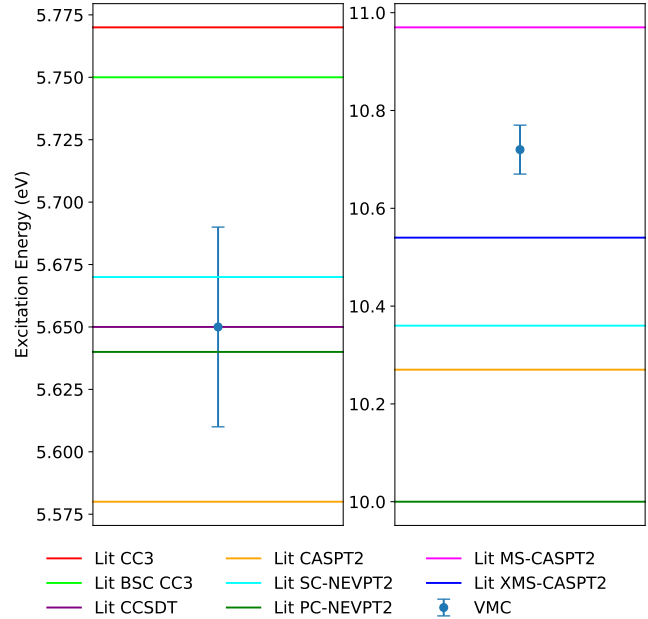


FIG. 4. Excitation energies in hexatriene and benzene in the left and right panels respectively. See also Table IV. In both molecules, the VMC used 500 determinants in ground state and 1000 for the excited state. Reference values for coupled cluster, CASPT2 and NEVPT2 are taken from the work of Loos and coworkers.<sup>20</sup>

TABLE IV. Excitation energies for hexatriene and benzene. The VMC uncertainties on the final digits are given in parentheses. The included literature<sup>20</sup> values use an aug-cc-pVQZ basis set for CC3 and CCSDT in hexatriene and an aug-cc-pVQZ basis set for all varieties of CASPT2 and NEVPT2, except for PC-NEVPT2 in benzene, which used aug-cc-pVTZ.

Method	Hexatriene	Benzene
VMC	5.65(4)	10.72(5)
CC3	5.77	
BSC CC3	5.75	
CCSDT	5.65	
CASPT2	5.58	10.27
PC-NEVPT2	5.64	10.00
SC-NEVPT2	5.67	10.36
MS-CASPT2		10.97
XMS-CASPT2		10.54

TABLE III. Excitation energies for the carbon trimer and nitrosomethane. The VMC uncertainties on the final digits are given in parentheses. The included literature<sup>20</sup> values use an aug-cc-pVQZ basis set for the carbon trimer and the CC3 and CASPT2 values for nitrosomethane. The literature nitrosomethane CCSDT and sCI results used an aug-cc-pVTZ basis set.

Method	Carbon Trimer	Nitrosomethane
VMC	5.90(4)	4.79(7)
CC3	7.22	5.74
CCSDT	6.58	5.29
CASPT2	5.82	4.78
sCI	5.86	4.76
Lit TBE	5.86	4.74

For molecules at the scale of hexatriene and benzene, high accuracy excitation energies from sCI are now unaffordable and various flavors of coupled cluster and multireference perturbation theory are left as the main quantum chemistry tools. This leaves space for our VMC approach to provide reliable excitation energies that can help determine whichever other methods are most accurate in larger systems. For the hexatriene results shown in the left panel of Figure 4 and Table IV, we see that VMC is in closer agreement with coupled cluster, particularly CCSDT, instead of CASPT2. This aligns with the conclusions of Loos and coworkers that the  $2^1A_g$  state has a high level of singles character, making coupled cluster with triples more reliable than it is for pure double excitations. In

the case of the  $2^1A_{1g}$  state in benzene, the literature<sup>20</sup> values consist only of different varieties of CASPT2 and NEVPT2, which show a significant spread of almost an entire eV in their excitation energy predictions without an obvious reason to favor any particular value. Our VMC result lands closest to the XMS-CASPT2 value, but is higher by about 0.18 eV and it may serve as a useful point of comparison for any other methods that are applied to this state in the future.

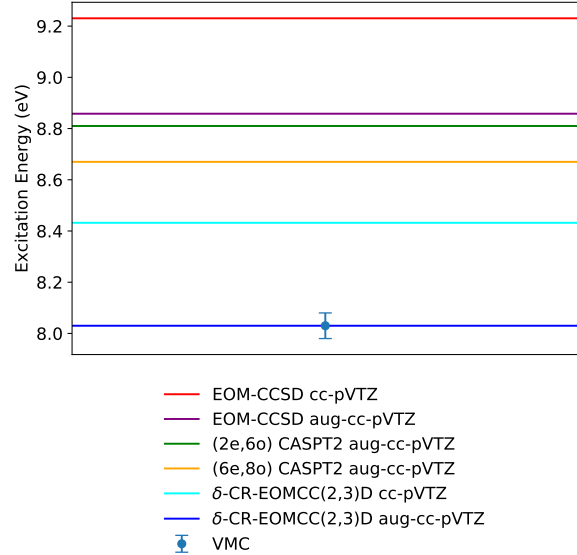


FIG. 5. Excitation energy of the lowest CT state in ammonia-difluorine for VMC and quantum chemistry approaches. See also Table V. The VMC used 300 determinants in the ground state and 500 for the excited state.

#### D. Charge Transfer: Ammonia-difluorine

With the accuracy of our method well established for valence single excitations and double excitations, we now show the same holds true for charge transfer states using the well-known ammonia-difluorine test system<sup>37,38,124,125</sup> at a separation of 6 Å. Our wave function generation proceeds as before with a (2e,6o) active space for the SS-CASSCF and a (22e,40o) space for the sCI using pseudopotentials and an aug-cc-pVTZ basis set.<sup>120</sup> For comparison to our VMC, we performed  $\delta$ -CR-EOMCC(2,3)D<sup>126</sup> calculations in GAMESS<sup>123</sup> and EOM-CCSD and CASPT2 calculations in Molpro.<sup>122</sup>

From Figure 5 and Table V, we see that our VMC is in excellent agreement with the aug-cc-pVTZ  $\delta$ -CR-EOMCC(2,3)D result. With only a cc-pVTZ basis set, the  $\delta$ -CR-EOMCC(2,3)D excitation energy is 0.4 eV larger and EOM-CCSD has a substantial error of about 0.8 eV even with augmentation, showing the importance of both including some triples in the coupled cluster and using diffuse functions for quantitative accuracy. We also note that CASPT2 with a (2e,6o) active space, a 6 state state-average (necessary to even see the CT state), and IPEA shift of 0.25 has an error comparable to EOM-CCSD's, while increasing the active space to (6e,8o) with the same state averaging and shift improves the accuracy by only 0.14 eV. CASPT2's difficulties are likely due to the limitations of state-averaging for CT states, which we can avoid through our state-specific methodology. The high accuracy of our VMC in this CT example indicates that we can obtain reliable excitation energies regardless of the type of excited state, a versatility that neither coupled cluster nor CASPT2 can achieve.

TABLE V. Excitation energies for the CT state in ammonia-difluorine. The VMC uncertainty for the last digit is given in parentheses.

Method	Excitation Energy (eV)
VMC	8.03(5)
(2e,6o) CASPT2 aug-cc-pVTZ	8.81
(6e,8o) CASPT2 aug-cc-pVTZ	8.67
CCSD cc-pVTZ	9.23
CCSD aug-cc-pVTZ	8.86
$\delta$ -CR-EOMCC(2,3)D cc-pVTZ	8.43
$\delta$ -CR-EOMCC(2,3)D aug-cc-pVTZ	8.03

#### E. Larger Systems: Uracil and Tetrafluorethylene-ethylene

We have demonstrated our approach's high level of accuracy across multiple types of excited states and now apply it to two larger molecules. We first address the  $2^1A'$  and  $3^1A'$  states in uracil, which appear as part of the Thiel set<sup>26</sup> and other benchmarking studies.<sup>127,128</sup> To generate our ansatzes, we used a (10e,8o) active space for the SS-CASSCF and a (42e,42o) space for the sCI with pseudopotentials and a cc-pVTZ basis set.<sup>120</sup>

These states have been previously studied with different levels of coupled cluster and CASPT2, giving a significant range of answers that spans 0.7 eV for the  $2^1A'$  state and almost an entire eV for the  $3^1A'$  state. The latter state is notable for having a significant, though non-dominant, amount of double excitation character, in the range of 15 to 20 percent based on CASSCF analysis, which might lead to hesitation

over whether to trust coupled cluster or CASPT2. VMC is in a position to provide the necessary guidance, with our results ending up in good agreement with the CCSD(T) results of Szalay and coworkers<sup>128</sup> for both states and more generally supporting the higher excitation energy predictions of coupled cluster over the CASPT2 results of Roos<sup>127</sup> and Thiel.<sup>26</sup> We also note that while the numbers of determinants needed in VMC after systematic expansion are larger than those used for smaller molecules, they can remain modestly sized due to the error cancellation benefits of our variance matching procedure.

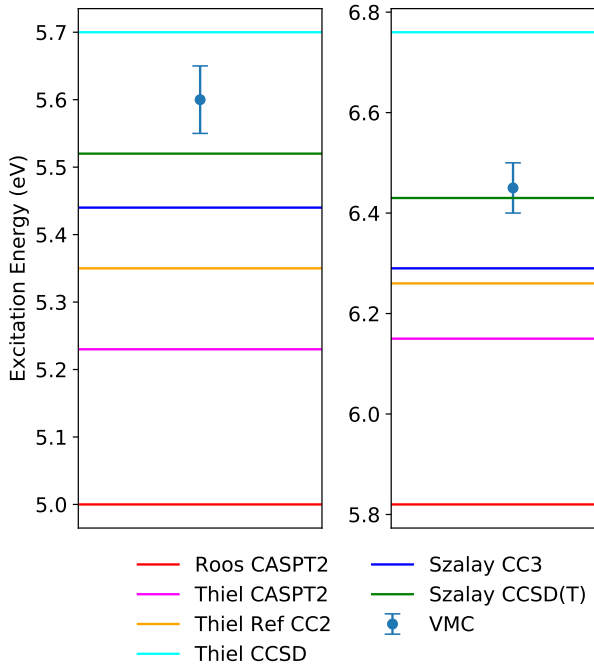


FIG. 6. Excitation energies in uracil. The left panel depicts values for the  $2\ 1A'$  state and the right panel for the  $3\ 1A'$  state. See also Table VI. The VMC used 500 determinants the ground state and 1500 for each of the excited states.

TABLE VI. Excitation energies in eV for the  $2\ 1A'$  and  $3\ 1A'$  states in uracil. The VMC uncertainty for the last digit is given in parentheses. The literature results from Thiel<sup>26</sup> and Szalay<sup>128</sup> used a TZVP basis set, with the Thiel set using an aug-cc-pVQZ CC2 result as its reference. Details on the ANO type basis set used by Roos can be found in the original paper.<sup>127</sup>

Method	$2\ 1A'$	$3\ 1A'$
VMC	5.60(5)	6.45(5)
Roos CASPT2	5.00	5.82
Thiel Ref CC2	5.35	6.26
Thiel CCSD	5.70	6.76
Thiel CASPT2	5.23	6.15
Szalay CC3	5.44	6.29
Szalay CCSD(T)	5.52	6.43

Our final system is the tetrafluoroethylene-ethylene charge transfer test system<sup>4,37,38,129–134</sup> at a separation of 5 Å. We

used a (4e,3o) active space for the SS-CASSCF followed by a (48e,50o) space for the sCI with pseudopotentials and an aug-cc-pVTZ basis set.<sup>120</sup> As with the ammonia-difluorine CT state, we again compare our VMC results to EOM-CCSD, CASPT2, and  $\delta$ -CR-EOMCC(2,3)D. Due to the size of system, we obtained only an approximate  $\delta$ -CR-EOMCC(2,3)D value at the aug-cc-pVTZ level by applying a basis set correction to the aug-cc-pVDZ value based on the difference between the EOM-CCSD excitation energies for those two basis sets. The excited state VMC optimization in this system was particularly challenging and produced an optimization history that did not offer a clear linear trend of energy vs variance with which to make our extrapolation to variance match with the ground state. Thus, in this system, we instead performed the extrapolation based on the ground state optimization history. With these nuances in mind, we still find good agreement between VMC and  $\delta$ -CR-EOMCC(2,3)D, while CASPT2 with a (4e,3o) space, 3 state state-average, and IPEA shift of 0.25 produces a significant error of around 0.8 eV. CASPT2's underestimation of the excitation energy in this system while overestimating for ammonia-difluorine reflects the unsystematic nature of its state-averaging-induced errors in CT states, in contrast to coupled cluster's strong tendency to error high for double excitations, particularly pure ones. We also note that use of augmented basis sets is essential for quantitative accuracy in this test system, with the coupled cluster values in Table VII showing errors of well over an eV when diffuse functions are absent. Our results reinforce our earlier conclusions from ammonia-difluorine that VMC can avoid the pitfalls of state-averaging for CT states, now in a large system and basis set where the highest orders of coupled cluster are computationally infeasible.

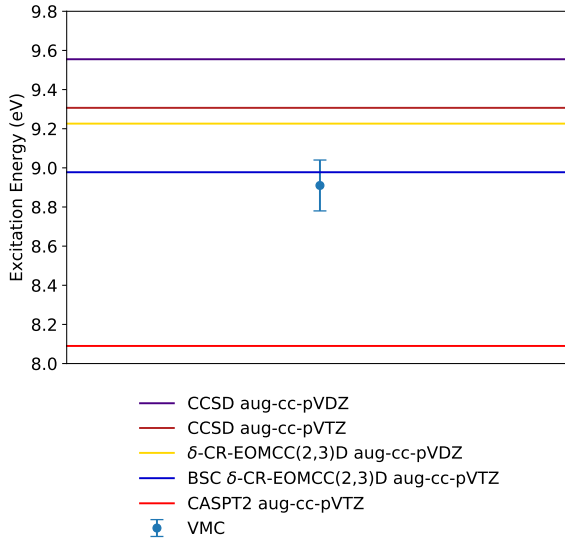


FIG. 7. Excitation energy of the lowest CT state in tetrafluoroethylene-ethylene for VMC and quantum chemistry approaches. See also Table VII. The VMC used 500 determinants the ground state and 1500 for the excited state.

TABLE VII. Excitation energies for the CT state in tetrafluoroethylene-ethylene. The VMC uncertainty for the final digits is given in parentheses.

Method	Excitation Energy (eV)
VMC	8.91(13)
CASPT2 aug-cc-pVTZ	8.09
CCSD cc-pVDZ	11.15
CCSD cc-pVTZ	10.57
CCSD aug-cc-pVDZ	9.56
CCSD aug-cc-pVTZ	9.31
δ-CR-EOMCC(2,3)D cc-pVDZ	10.55
δ-CR-EOMCC(2,3)D aug-cc-pVDZ	9.23
BSC δ-CR-EOMCC(2,3)D aug-cc-pVTZ	8.98

#### IV. CONCLUSIONS

By constructing a method that combines the advantages of SS-CASSCF, sCI, and VMC, we find that it is possible to offer high accuracy excitation energy predictions across singly excited, doubly excited, and charge transfer states. Unlike CASPT2, this combined method avoids state averaging and is thus able to accommodate the post-excitation orbital relaxations that are so crucial in charge transfer. Unlike EOM-CC, the method is explicitly multi-configurational, making it much more reliable in doubly excited states. Unlike sCI on its own, the method is able to arrive at accurate excitation energies with much shorter determinant expansions thanks to the combined effect of Jastrow factors and variance matching. Together, these advantages allow the method to make reliable excitation energy predictions in a wider variety of excited states than

either coupled cluster or multi-reference perturbation theory while also reaching into system sizes beyond the current limits of sCI without sacrificing basis set quality. In key systems like uracil and tetrafluoroethylene-ethylene, agreement between our method and the highest level coupled cluster that can be afforded allows us to make excitation energy predictions with a confidence that is bolstered by the significant differences in these methods' underlying approximations.

From a methodological perspective, our key finding is that SS-CASSCF orbitals are accurate enough that further optimization within VMC is not necessary for producing accurate excitation energies. The practical advantage of this finding is that, while more efficient than it used to be, orbital optimization within VMC remains more difficult than CI coefficient and Jastrow optimization, and by avoiding it we can therefore reduce computational cost. We also find that, in most cases, effective variance matching can be performed without the need for interpolations based on multiple wave function expansion lengths by instead using linear extrapolations based on optimization history. Finally, removing low-priority parameters from the blocked linear method steps while still optimizing them with accelerated descent did not prevent high accuracies from being attained, which allows us to work with smaller sample sizes than would otherwise be necessary when estimating the elements of the linear method matrices.

Looking forward, we note that our VMC approach can be applied to additional excited state situations beyond those considered in this work. Core excitations are one area where VMC has already demonstrated high accuracy,<sup>88</sup> and work is currently underway on exploring whether the approach presented here will offer similar benefits in that context. Excited state absorption<sup>135</sup> is another setting that challenges both CASPT2 and coupled cluster and where the present approach could be usefully applied without any obvious additional difficulty. Finally, in solid-state systems, the discrete states of defects are another potential opportunity for applying our state-specific machinery. Methodologically, further improvements in user-accessibility remain an ongoing effort. Systematic determination and automation of effective choices in optimization details such as the mixture between accelerated descent and the blocked linear method, descent hyperparameters, and the choice of guiding function should streamline workflows in future. With such improvements, it should be possible to apply our SS-CASSCF/sCI/VMC methodology to an even wider range of challenging excited state questions.

#### ACKNOWLEDGMENTS

This work was supported by the Office of Science, Office of Basic Energy Sciences, the U.S. Department of Energy, Contract No. DE-AC02-05CH11231. Computational work was performed with the Berkeley Research Computing Savio cluster, the LBNL Lawrencium cluster, and the National Energy Research Scientific Computing Center, a DOE Office of Science User Facility supported by the Office of Science of the U.S. Department of Energy under Contract No. DE-AC02-05CH11231.

## Appendix A: Molecular Geometries

TABLE VIII. Structure of thioformaldehyde. Coordinates in Å.

C	0.000 000	0.000 000	-1.104 273
S	0.000 000	0.000 000	0.514 631
H	0.000 000	0.918 957	-1.677 563
H	0.000 000	-0.918 957	-1.677 563

TABLE IX. Structure of methanimine. Coordinates in Å.

C	0.056 604	0.000 000	0.587 869
N	0.056 961	0.000 000	-0.686 225
H	-0.842 138	0.000 000	1.202 802
H	1.007 951	0.000 000	1.108 065
H	-0.899 369	0.000 000	-1.038 338

TABLE X. Structure of ketene. Coordinates in Å.

C	0.000 000	0.000 000	-1.295 479
C	0.000 000	0.000 000	0.018 514
O	0.000 000	0.000 000	1.183 578
H	0.000 000	0.938 930	-1.818 814
H	0.000 000	-0.938 930	-1.818 814

TABLE XI. Structure of carbon trimer. Coordinates in Å.

C	0.000 000	0.000 000	0.000 000
C	0.000 000	0.000 000	1.298 313
C	0.000 000	0.000 000	-1.298 313

TABLE XII. Structure of nitrosomethane. Coordinates in Å.

C	-0.944 193	0.000 000	-0.567 405
N	-0.002 867	0.000 000	0.571 831
O	1.157 919	0.000 000	0.229 939
H	-0.409 287	0.000 000	-1.515 646
H	-1.574 151	0.882 677	-0.457 339
H	-1.574 151	-0.882 677	-0.457 339

TABLE XIII. Structure of hexatriene. Coordinates in Å.

C	-0.000 131	0.672 998	0.000 000
C	0.000 131	-0.672 998	0.000 000
C	1.201 720	1.480 569	0.000 000
C	-1.201 720	-1.480 569	0.000 000
C	1.201 720	2.821 239	0.000 000
C	-1.201 720	-2.821 239	0.000 000
H	-0.949 240	1.200 063	0.000 000
H	0.949 240	-1.200 063	0.000 000
H	2.145 737	0.948 370	0.000 000
H	-2.145 737	-0.948 370	0.000 000
H	0.274 043	3.378 403	0.000 000
H	-0.274 043	-3.378 403	0.000 000
H	2.122 561	3.385 081	0.000 000
H	-2.122 561	-3.385 081	0.000 000

TABLE XIV. Structure of benzene. Coordinates in Å.

C	0.000 000	1.392 503	0.000 000
C	-1.205 943	0.696 252	0.000 000
C	-1.205 943	-0.696 252	0.000 000
C	0.000 000	-1.392 503	0.000 000
C	1.205 943	-0.696 252	0.000 000
C	1.205 943	0.696 252	0.000 000
H	-2.141 717	1.236 521	0.000 000
H	-2.141 717	-1.236 521	0.000 000
H	0.000 000	-2.473 041	0.000 000
H	2.141 717	-1.236 521	0.000 000
H	2.141 717	1.236 521	0.000 000
H	0.000 000	2.473 041	0.000 000

TABLE XV. Structure of ammonia-fluorine. Coordinates in Å.

N	0.000 000	-0.234 913	-3.520 527
H	0.000 000	0.704 739	-3.904 943
H	0.813 763	-0.704 739	-3.904 943
H	-0.813 763	-0.704 739	-3.904 943
F	0.000 000	-0.234 913	2.479 473
F	0.000 000	-0.234 913	3.904 943

TABLE XVI. Structure of uracil. Coordinates in Å.

H	-2.025 413	-1.517 742	0.000 000
H	-0.021 861	1.995 767	0.000 000
H	2.182 391	-1.602 586	0.000 000
H	-0.026 659	-2.791 719	0.000 000
C	-1.239 290	0.359 825	0.000 000
C	1.279 718	0.392 094	0.000 000
C	1.243 729	-1.064 577	0.000 000
C	0.055 755	-1.709 579	0.000 000
O	-2.308 803	0.954 763	0.000 000
O	2.287 387	1.092 936	0.000 000
N	-1.139 515	-1.026 364	0.000 000
N	0.000 000	0.978 951	0.000 000

TABLE XVII. Structure of tetrafluorethylene-ethylene. Coordinates in Å.

F	-1.394866	-1.110938	-1.070259
F	-1.394866	1.110938	-1.070259
F	1.394866	-1.110938	-1.070259
F	1.394866	1.110938	-1.070259
C	-0.667784	0.000000	-1.088369
C	0.667784	0.000000	-1.088369
H	-1.244242	0.935429	3.830123
H	-1.244242	-0.935429	3.830123
H	1.244242	0.935429	3.830123
H	1.244242	-0.935429	3.830123
C	-0.674558	0.000000	3.833889
C	0.674558	0.000000	3.833889

## Appendix B: Optimization Details

As discussed in the main text, we perform all our VMC optimizations with the hybrid method, alternating between sections of AD and blocked LM optimization. Each AD portion of a hybrid macro-iteration produces 5 vectors of parameter differences as input to the blocked LM algorithm as parameter coupling information.<sup>101</sup> As mentioned in section IIB, all blocked LM iterations divided a filtered parameter set into 5 blocks and retained 30 parameter directions for the second stage of the algorithm. In practice, shift values<sup>118</sup>  $c_i$  and  $c_s$  are added to blocked LM matrices to prevent unwisely large steps in parameter space. Our implementation of the LM uses an adaptive scheme<sup>101</sup> that compares target function values calculated through correlated sampling for three different sets of shift values and selects whichever update step and corresponding shifts give the lowest target function. For all optimizations, we set the initial values of  $c_i$  and  $c_s$  to 0.1 and 1.0 respectively.

The particular numbers of macro-iterations and samples for each molecule are listed in Table XVIII and Table XIX gives details on the uncertainties resulting from the variance matching extrapolation procedure that we have used for all our excitation energy results. In Table XIX, the energy-variance slope used for nitrosomethane is significantly smaller than the others due to the optimization starting from a preoptimized wave function, and unlike the other cases, the slope used for tetrafluoroethylene-ethylene is based on the ground state optimization instead of excited state data.

TABLE XVIII. Macro-iterations used for GS and ES optimizations. Samples per iteration used for AD and blocked LM portions of the hybrid optimizations. Total samples for AD and LM with the costs for GS and ES combined. The nominal samples per iteration for blocked LM iterations is multiplied by 3 for computing the total sampling effort due to the need to run over the samples additional times to perform the automated parameter selection and the blocked LM algorithm.

Molecule	Macro-iterations: (GS, ES)	Samples per iteration: (AD, LM)	Total Samples (10 <sup>6</sup> ): (AD, LM)
Thioformaldehyde	(7,8)	(3 × 10 <sup>4</sup> , 1 × 10 <sup>6</sup> )	(111, 135)
Methanimine	(5,6)	(3 × 10 <sup>4</sup> , 1 × 10 <sup>6</sup> )	(99, 99)
Ketene	(6,8)	(3 × 10 <sup>4</sup> , 1 × 10 <sup>6</sup> )	(108, 126)
Carbon trimer	(5,5)	(3 × 10 <sup>4</sup> , 1 × 10 <sup>6</sup> )	(96, 99)
Nitrosomethane	(7,6)	(3 × 10 <sup>4</sup> , 1 × 10 <sup>6</sup> )	(105, 117)
Hexatriene	(8,8)	(3 × 10 <sup>4</sup> , 1 × 10 <sup>6</sup> )	(114, 144)
Benzene	(7,7)	(3 × 10 <sup>4</sup> , 1 × 10 <sup>6</sup> )	(108, 126)
Ammonia-difluorine	(4,6)	(3 × 10 <sup>4</sup> , 1 × 10 <sup>6</sup> )	(96, 90)
Uracil 2 <sup>1</sup> A'	(7,8)	(5 × 10 <sup>4</sup> , 1 × 10 <sup>6</sup> )	(104, 135)
Uracil 3 <sup>1</sup> A'	(7,8)	(5 × 10 <sup>4</sup> , 1 × 10 <sup>6</sup> )	(104, 135)
Tetrafluoroethylene-ethylene	(6,7)	(5 × 10 <sup>4</sup> , 1 × 10 <sup>6</sup> )	(175, 117)

TABLE XIX. Uncertainties in the excitation energies due to stochastic averaging and variance matching extrapolation. Raw variance values for ground and excited states. Energy-variance slopes used in the extrapolations and uncertainties in the slopes due to the uncertainty in the individual blocked LM optimization points.

Molecule	Excitation Energy (eV)	Averaging Uncertainty (eV)	Extrapolation Uncertainty (eV)	GS Variance (a.u.)	ES Variance (a.u.)	Slope (a.u.)	Slope Uncertainty (a.u.)
Thioformaldehyde	2.28	0.02	0.001	0.178	0.177	0.4936	0.052
Methanimine	5.13	0.02	0.01	0.216	0.235	0.3727	0.026
Ketene	3.91	0.02	0.04	0.456	0.494	0.3924	0.039
Carbon trimer	5.90	0.02	0.02	0.209	0.195	0.5360	0.046
Nitrosomethane	4.79	0.03	0.04	0.527	0.563	0.0480	0.037
Hexatriene	5.65	0.03	0.01	0.605	0.591	0.5574	0.012
Benzene	10.72	0.03	0.02	0.570	0.600	0.4317	0.022
Ammonia-difluorine	8.03	0.03	0.02	1.066	1.102	0.3977	0.024
Uracil 2 <sup>1</sup> A'	5.60	0.04	0.01	1.393	1.406	0.5165	0.027
Uracil 3 <sup>1</sup> A'	6.45	0.04	0.01	1.393	1.405	0.4622	0.015
Tetrafluoroethylene-ethylene	8.91	0.05	0.08	2.354	2.689	0.2151	0.009

<sup>1</sup>M. Casida and M. Huix-Rotllant, "Progress in time-dependent density-functional theory," *Annual Review of Physical Chemistry* **63**, 287–323 (2012), pMID: 22242728, <https://doi.org/10.1146/annurev-physchem-032511-143803>.

<sup>2</sup>N. T. Maitra, F. Zhang, R. J. Cave, and K. Burke, "Double excitations within time-dependent density functional theory linear response," *The Journal of Chemical Physics* **120**, 5932–5937 (2004), <https://doi.org/10.1063/1.1651060>.

<sup>3</sup>B. G. Levine, C. Ko, J. Quenneville, and T. J. Martínez, "Conical intersections and double excitations in time-dependent density functional theory," *Molecular Physics* **104**, 1039–1051 (2006), <https://doi.org/10.1080/00268970500417762>.

<sup>4</sup>A. Dreuw, J. L. Weisman, and M. Head-Gordon, "Long-range charge-transfer excited states in time-dependent density functional theory require non-local exchange," *The Journal of Chemical Physics* **119**, 2943–2946 (2003), <https://doi.org/10.1063/1.1590951>.

<sup>5</sup>A. Dreuw and M. Head-Gordon, "Failure of time-dependent density functional theory for long-range charge-transfer excited states: The zincbacteriochlorin-bacteriochlorin and bacteriochlorophyll-spheroidene complexes," *Journal of the American Chemical Society* **126**, 4007–4016 (2004), pMID: 15038755, <https://doi.org/10.1021/ja039556n>.

<sup>6</sup>P. Elliott, S. Goldson, C. Canahui, and N. T. Maitra, "Perspectives on double-excitations in tddft," *Chemical Physics* **391**, 110–119 (2011), open problems and new solutions in time dependent density functional theory.

<sup>7</sup>N. T. Maitra, "Charge transfer in time-dependent density functional theory," **29**, 423001 (2017).

<sup>8</sup>D. Hait and M. Head-Gordon, "Excited state orbital optimization via minimizing the square of the gradient: General approach and application to singly and doubly excited states via density functional theory," *Journal of Chemical Theory and Computation* **16**, 1699–1710 (2020), pMID: 32017554, <https://doi.org/10.1021/acs.jctc.9b01127>.

<sup>9</sup>D. Hait and M. Head-Gordon, "Orbital optimized density functional theory for electronic excited states," *The Journal of Physical Chemistry Letters* **12**, 4517–4529 (2021), pMID: 33961437, <https://doi.org/10.1021/acs.jpclett.1c00744>.

<sup>10</sup>N. Mardirossian and M. Head-Gordon, "Thirty years of density functional theory in computational chemistry: an overview and extensive assessment of 200 density functionals," *Molecular Physics* **115**, 2315–2372 (2017), <https://doi.org/10.1080/00268976.2017.1333644>.

<sup>11</sup>A. D. Laurent and D. Jacquemin, "Td-dft benchmarks: A review," *International Journal of Quantum Chemistry* **113**, 2019–2039 (2013), <https://onlinelibrary.wiley.com/doi/pdf/10.1002/qua.24438>.

<sup>12</sup>K. L. Bak, P. Jørgensen, J. Olsen, T. Helgaker, and W. Klopfer, "Accuracy of atomization energies and reaction enthalpies in standard and extrapolated electronic wave function/basis set calculations," *The Journal of Chemical Physics* **112**, 9229–9242 (2000), <https://doi.org/10.1063/1.481544>.

<sup>13</sup>S. Coriani, D. Marchesan, J. Gauss, C. Hättig, T. Helgaker, and P. Jørgensen, "The accuracy of ab initio molecular geometries for systems containing second-row atoms," *The Journal of Chemical Physics* **123**, 184107 (2005), <https://doi.org/10.1063/1.2104387>.

<sup>14</sup>R. J. Bartlett and M. Musiał, "Coupled-cluster theory in quantum chemistry," *Rev. Mod. Phys.* **79**, 291–352 (2007).

<sup>15</sup>J. F. Stanton and R. J. Bartlett, "The equation of motion coupled-cluster method. a systematic biorthogonal approach to molecular excitation energies, transition probabilities, and excited state properties," *The Journal of Chemical Physics* **98**, 7029–7039 (1993), <https://doi.org/10.1063/1.464746>.

<sup>16</sup>D. Kánnár and P. G. Szalay, "Benchmarking coupled cluster methods on valence singlet excited states," *Journal of Chemical Theory and Computation* **10**, 3757–3765 (2014), pMID: 26588520, <https://doi.org/10.1021/ct500495n>.

<sup>17</sup>P.-F. Loos, A. Scemama, A. Blondel, Y. Garniron, M. Caffarel, and D. Jacquemin, "A mountaineering strategy to excited states: Highly accurate reference energies and benchmarks," *Journal of Chemical Theory and Computation* **14**, 4360–4379 (2018), pMID: 29966098, <https://doi.org/10.1021/acs.jctc.8b00406>.

<sup>18</sup>S. Hirata, M. Nooijen, and R. J. Bartlett, "High-order determinantal equation-of-motion coupled-cluster calculations for electronic excited states," *Chemical Physics Letters* **326**, 255 – 262 (2000).

<sup>19</sup>M. A. Watson and G. K.-L. Chan, "Excited states of butadiene to chemical accuracy: Reconciling theory and experiment," *J. Chem. Theory Comput.* **8**, 4013–4018 (2012), pMID: 26605568, <https://doi.org/10.1021/ct300591z>.

<sup>20</sup>P.-F. Loos, M. Boggio-Pasqua, A. Scemama, M. Caffarel, and D. Jacquemin, "Reference energies for double excitations," *J. Chem. Theory Comput.* **15**, 1939–1956 (2019), <https://doi.org/10.1021/acs.jctc.8b01205>.

<sup>21</sup>L. Serrano-Andrés, M. Merchán, I. Nebot-Gil, R. Lindh, and B. O. Roos, "Towards an accurate molecular orbital theory for excited states: Ethene, butadiene, and hexatriene," *The Journal of Chemical Physics* **98**, 3151–3162 (1993), <https://doi.org/10.1063/1.465071>.

<sup>22</sup>L. Serrano-Andrés, M. Merchán, M. Fülscher, and B. O. Roos, "A theoretical study of the electronic spectrum of thiophene," *Chemical Physics Letters* **211**, 125 – 134 (1993).

<sup>23</sup>K. Nakayama, H. Nakano, and K. Hirao, "Theoretical study of the  $\pi \rightarrow \pi^*$  excited states of linear polyenes: The energy gap between 1 1bu+ and 2 1ag states and their character," *International Journal of Quantum Chemistry* **66**, 157–175 (1998).

<sup>24</sup>B. Ostožić and W. Domcke, "Ab initio investigation of the potential energy surfaces involved in the photophysics of s-trans-1,3-butadiene," *Chemical Physics* **269**, 1 – 10 (2001).

<sup>25</sup>M. Dallos and H. Lischka, "A systematic theoretical investigation of the lowest valence- and Rydberg-excited singlet states of trans-butadiene. The character of the 11Bu (V) state revisited," *Theoretical Chemistry Accounts* **112**, 16–26 (2004).

<sup>26</sup>M. Schreiber, M. R. Silva-Junior, S. P. A. Sauer, and W. Thiel, "Benchmarks for electronically excited states: Caspt2, cc2, cc3d, and cc3," *J. Chem. Phys.* **128**, 134110 (2008), <https://doi.org/10.1063/1.2889385>.

<sup>27</sup>M. R. Silva-Junior, M. Schreiber, S. P. A. Sauer, and W. Thiel, "Benchmarks of electronically excited states: Basis set effects on caspt2 results," *J. Chem. Phys.* **133**, 174318 (2010), <https://doi.org/10.1063/1.3499598>.

<sup>28</sup>S. Duman, Y. Cakmak, S. Kolemen, E. U. Akkaya, and Y. Dede, "Heavy atom free singlet oxygen generation: Doubly substituted configurations dominate s1 states of bis-bodipys," *The Journal of Organic Chemistry* **77**, 4516–4527 (2012), pMID: 22530939, <https://doi.org/10.1021/jo300051v>.

<sup>29</sup>J. Wen, B. Han, Z. Havlas, and J. Michl, "An ms-caspt2 calculation of the excited electronic states of an axial difluoroborondipyrromethene (bodipy) dimer," *Journal of Chemical Theory and Computation* **14**, 4291–4297 (2018), pMID: 29874458, <https://doi.org/10.1021/acs.jctc.8b00136>.

<sup>30</sup>C. Rauer, J. J. Nogueira, P. Marquetand, and L. González, "Cyclobutane thymine photodimerization mechanism revealed by nonadiabatic molecular dynamics," *Journal of the American Chemical Society* **138**, 15911–15916 (2016), pMID: 27682199, <https://doi.org/10.1021/jacs.6b06701>.

<sup>31</sup>N. Ben Amor, A. Soupart, and M. C. Heitz, "Methodological CASPT2 study of the valence excited states of an iron-porphyrin complex," *Journal of Molecular Modeling* **23** (2017), 10.1007/s00894-017-3226-y.

<sup>32</sup>P.-F. Loos, F. Lipparini, M. Boggio-Pasqua, A. Scemama, and D. Jacquemin, "A mountaineering strategy to excited states: Highly accurate energies and benchmarks for medium sized molecules," *Journal of Chemical Theory and Computation* **16**, 1711–1741 (2020), pMID: 31986042, <https://doi.org/10.1021/acs.jctc.9b01216>.

<sup>33</sup>H. Werner and W. Meyer, "A quadratically convergent mcscf method for the simultaneous optimization of several states," *The Journal of Chemical Physics* **74**, 5794–5801 (1981), <https://doi.org/10.1063/1.440892>.

<sup>34</sup>A. Domingo, M. Á. Carvajal, C. de Graaf, K. Sivalingam, F. Neese, and C. Angeli, "Metal-to-metal charge-transfer transitions: reliable excitation energies from ab initio calculations," *Theoretical Chemistry Accounts* **131**, 1264 (2012).

<sup>35</sup>B. Meyer, A. Domingo, T. Krah, and V. Robert, "Charge transfer processes: the role of optimized molecular orbitals," *Dalton Trans.* **43**, 11209–11215 (2014).

<sup>36</sup>L. N. Tran, J. A. R. Shea, and E. Neuscamman, "Tracking excited states in wave function optimization using density matrices and variational principles," *J. Chem. Theory Comput.* **15**, 4790–4803 (2019), pMID: 31393725, <https://doi.org/10.1021/acs.jctc.9b00351>.

<sup>37</sup>A. K. Dutta, M. Nooijen, F. Neese, and R. Izsák, "Exploring the accuracy of a low scaling similarity transformed equation of motion method for vertical excitation energies," *Journal of Chemical Theory and Computation* **14**, 72–91 (2018), pMID: 29206453,

[https://doi.org/10.1021/acs.jctc.7b00802.](https://doi.org/10.1021/acs.jctc.7b00802)

<sup>38</sup>B. Kozma, A. Tajti, B. Demoulin, R. Izsák, M. Nooijen, and P. G. Szalay, “A new benchmark set for excitation energy of charge transfer states: Systematic investigation of coupled cluster type methods,” *Journal of Chemical Theory and Computation* **16**, 4213–4225 (2020), pMID: 32502351, <https://doi.org/10.1021/acs.jctc.0c00154>.

<sup>39</sup>P.-F. Loos, M. Comin, X. Blase, and D. Jacquemin, “Reference energies for intramolecular charge-transfer excitations,” *Journal of Chemical Theory and Computation* **17**, 3666–3686 (2021), pMID: 33955742, <https://doi.org/10.1021/acs.jctc.1c00226>.

<sup>40</sup>J. J. Eriksen, T. A. Anderson, J. E. Deustua, K. Ghanem, D. Hait, M. R. Hoffmann, S. Lee, D. S. Levine, I. Magoulas, J. Shen, N. M. Tubman, K. B. Whaley, E. Xu, Y. Yao, N. Zhang, A. Alavi, G. K.-L. Chan, M. Head-Gordon, W. Liu, P. Piecuch, S. Sharma, S. L. Ten-no, C. J. Umrigar, and J. Gauss, “The ground state electronic energy of benzene,” *The Journal of Physical Chemistry Letters* **11**, 8922–8929 (2020), pMID: 33022176, <https://doi.org/10.1021/acs.jpclett.0c02621>.

<sup>41</sup>J. J. Eriksen, “The shape of full configuration interaction to come,” *The Journal of Physical Chemistry Letters* **12**, 418–432 (2021), pMID: 33356287, <https://doi.org/10.1021/acs.jpclett.0c03225>.

<sup>42</sup>J. B. Schriber and F. A. Evangelista, “Adaptive configuration interaction for computing challenging electronic excited states with tunable accuracy,” *Journal of Chemical Theory and Computation* **13**, 5354–5366 (2017), pMID: 28892621, <https://doi.org/10.1021/acs.jctc.7b00725>.

<sup>43</sup>A. A. Holmes, C. J. Umrigar, and S. Sharma, “Excited states using semistochastic heat-bath configuration interaction,” *The Journal of Chemical Physics* **147**, 164111 (2017), <https://doi.org/10.1063/1.4998614>.

<sup>44</sup>A. D. Chien, A. A. Holmes, M. Otten, C. J. Umrigar, S. Sharma, and P. M. Zimmerman, “Excited states of methylene, polyenes, and ozone from heat-bath configuration interaction,” *The Journal of Physical Chemistry A* **122**, 2714–2722 (2018), pMID: 29473750, <https://doi.org/10.1021/acs.jpca.8b01554>.

<sup>45</sup>O. Legeza, J. Roder, and B. A. Hess, “Qc-dmrg study of the ionic-neutral curve crossing of lif,” *Molecular Physics* **101**, 2019–2028 (2003), <https://www.tandfonline.com/doi/pdf/10.1080/0026897031000155625>.

<sup>46</sup>S. Sharma, T. Yanai, G. H. Booth, C. J. Umrigar, and G. K.-L. Chan, “Spectroscopic accuracy directly from quantum chemistry: Application to ground and excited states of beryllium dimer,” *The Journal of Chemical Physics* **140**, 104112 (2014), <https://doi.org/10.1063/1.4867383>.

<sup>47</sup>G. H. Booth and G. K.-L. Chan, “Communication: Excited states, dynamic correlation functions and spectral properties from full configuration interaction quantum monte carlo,” *The Journal of Chemical Physics* **137**, 191102 (2012), <https://doi.org/10.1063/1.4766327>.

<sup>48</sup>A. Humeniuk and R. Mitrić, “Excited states from quantum monte carlo in the basis of slater determinants,” *The Journal of Chemical Physics* **141**, 194104 (2014), <https://doi.org/10.1063/1.4901020>.

<sup>49</sup>N. S. Blunt, S. D. Smart, G. H. Booth, and A. Alavi, “An excited-state approach within full configuration interaction quantum monte carlo,” *The Journal of Chemical Physics* **143**, 134117 (2015), <https://aip.scitation.org/doi/pdf/10.1063/1.4932595>.

<sup>50</sup>N. S. Blunt, A. Alavi, and G. H. Booth, “Krylov-projected quantum monte carlo method,” *Phys. Rev. Lett.* **115**, 050603 (2015).

<sup>51</sup>N. S. Blunt, G. H. Booth, and A. Alavi, “Density matrices in full configuration interaction quantum monte carlo: Excited states, transition dipole moments, and parallel distribution,” *The Journal of Chemical Physics* **146**, 244105 (2017), <https://doi.org/10.1063/1.4986963>.

<sup>52</sup>Y. Kurashige, G. K.-L. Chan, and T. Yanai, “Entangled quantum electronic wavefunctions of the mn4ca05 cluster in photosystem ii,” *Nature Chemistry* **5**, 660–666 (2013).

<sup>53</sup>F. Liu, Y. Kurashige, T. Yanai, and K. Morokuma, “Multireference ab initio density matrix renormalization group (dmrg)-casscf and dmrg-caspt2 study on the photochromic ring opening of spiropyran,” *Journal of Chemical Theory and Computation* **9**, 4462–4469 (2013), pMID: 26589164, <https://doi.org/10.1021/ct400707k>.

<sup>54</sup>S. Sharma, K. Sivalingam, F. Neese, and G. K.-L. Chan, “Low-energy spectrum of iron–sulfur clusters directly from many-particle quantum mechanics,” *Nature Chemistry* **6**, 927–933 (2014).

<sup>55</sup>D. S. Levine, D. Hait, N. M. Tubman, S. Lehtola, K. B. Whaley, and M. Head-Gordon, “Casscf with extremely large active spaces using the adaptive sampling configuration interaction method,” *Journal of Chemical Theory and Computation* **16**, 2340–2354 (2020), pMID: 32109055, <https://doi.org/10.1021/acs.jctc.9b01255>.

<sup>56</sup>W. Dobrutz, O. Weser, N. A. Bogdanov, A. Alavi, and G. Li Manni, “Spin-pure stochastic-casscf via guga-fciqmc applied to iron–sulfur clusters,” *Journal of Chemical Theory and Computation* **17**, 5684–5703 (2021), pMID: 34469685, <https://doi.org/10.1021/acs.jctc.1c00589>.

<sup>57</sup>M. Caffarel, T. Applencourt, E. Giner, and A. Scemama, “Communication: Toward an improved control of the fixed-node error in quantum monte carlo: The case of the water molecule,” *The Journal of Chemical Physics* **144**, 151103 (2016), <https://doi.org/10.1063/1.4947093>.

<sup>58</sup>A. Scemama, T. Applencourt, E. Giner, and M. Caffarel, “Accurate nonrelativistic ground-state energies of 3d transition metal atoms,” *The Journal of Chemical Physics* **141**, 244110 (2014), <https://doi.org/10.1063/1.4903985>.

<sup>59</sup>A. Scemama, A. Benali, D. Jacquemin, M. Caffarel, and P.-F. Loos, “Excitation energies from diffusion monte carlo using selected configuration interaction nodes,” *The Journal of Chemical Physics* **149**, 034108 (2018), <https://doi.org/10.1063/1.5041327>.

<sup>60</sup>A. Scemama, M. Caffarel, A. Benali, D. Jacquemin, and P.-F. Loos, “Influence of pseudopotentials on excitation energies from selected configuration interaction and diffusion monte carlo,” *Results in Chemistry* **1**, 100002 (2019).

<sup>61</sup>M. Dash, J. Feldt, S. Moroni, A. Scemama, and C. Filippi, “Excited states with selected configuration interaction-quantum monte carlo: Chemically accurate excitation energies and geometries,” *Journal of Chemical Theory and Computation* **15**, 4896–4906 (2019), pMID: 31348645, <https://doi.org/10.1021/acs.jctc.9b00476>.

<sup>62</sup>M. Dash, S. Moroni, C. Filippi, and A. Scemama, “Tailoring cipsi expansions for qmc calculations of electronic excitations: The case study of thiophene,” *Journal of Chemical Theory and Computation* **17**, 3426–3434 (2021), pMID: 34029098, <https://doi.org/10.1021/acs.jctc.1c00212>.

<sup>63</sup>A. Benali, K. Gasperich, K. D. Jordan, T. Applencourt, Y. Luo, M. C. Bennett, J. T. Krogel, L. Shulenburger, P. R. C. Kent, P.-F. Loos, A. Scemama, and M. Caffarel, “Toward a systematic improvement of the fixed-node approximation in diffusion monte carlo for solids—a case study in diamond,” *The Journal of Chemical Physics* **153**, 184111 (2020), <https://doi.org/10.1063/5.0021036>.

<sup>64</sup>C. J. Umrigar, K. G. Wilson, and J. W. Wilkins, “Optimized trial wave functions for quantum monte carlo calculations,” *Phys. Rev. Lett.* **60**, 1719–1722 (1988).

<sup>65</sup>N. D. Drummond, M. D. Towler, and R. J. Needs, “Jastrow correlation factor for atoms, molecules, and solids,” *Phys. Rev. B* **70**, 235119 (2004).

<sup>66</sup>P. López Ríos, P. Seth, N. D. Drummond, and R. J. Needs, “Framework for constructing generic jastrow correlation factors,” *Phys. Rev. E* **86**, 036703 (2012).

<sup>67</sup>A. Lüchow, A. Sturm, C. Schulte, and K. Haghghi Mood, “Generic expansion of the jastrow correlation factor in polynomials satisfying symmetry and cusp conditions,” *J. Chem. Phys.* **142**, 084111 (2015), <https://doi.org/10.1063/1.4909554>.

<sup>68</sup>C. J. Huang, C. J. Umrigar, and M. P. Nightingale, “Accuracy of electronic wave functions in quantum Monte Carlo: The effect of high-order correlations,” *J. Chem. Phys.* **107**, 3007–3013 (1997).

<sup>69</sup>M. Casula and S. Sorella, “Geminal wave functions with Jastrow correlation: A first application to atoms,” *J. Chem. Phys.* **119**, 6500–6511 (2003), arXiv:0305169v1 [arXiv:cond-mat].

<sup>70</sup>M. Casula, C. Attaccalite, and S. Sorella, “Correlated geminal wave function for molecules: An efficient resonating valence bond approach,” *J. Chem. Phys.* **121**, 7110–7126 (2004), <https://doi.org/10.1063/1.1794632>.

<sup>71</sup>F. Sterpone, L. Spanu, L. Ferraro, S. Sorella, and L. Guidoni, “Dissecting the hydrogen bond: A quantum monte carlo approach,” *J. Chem. Theory Comput.* **4**, 1428–1434 (2008), pMID: 26621429, <https://doi.org/10.1021/ct800121e>.

<sup>72</sup>T. D. Beaudet, M. Casula, J. Kim, S. Sorella, and R. M. Martin, “Molecular hydrogen adsorbed on benzene: Insights from a quantum Monte Carlo study,” *J. Chem. Phys.* **129**, 164711 (2008).

<sup>73</sup>M. Marchi, S. Azadi, M. Casula, and S. Sorella, “Resonating valence bond wave function with molecular orbitals: Application to first-row molecules,” *J. Chem. Phys.* **131**, 154116 (2009), <https://doi.org/10.1063/1.3249966>.

<sup>74</sup>A. Zen, Y. Luo, G. Mazzola, L. Guidoni, and S. Sorella, “Ab initio molecular dynamics simulation of liquid water by quantum Monte Carlo,” *J.*

Chem. Phys. **142**, 144111 (2015).

<sup>75</sup>B. V. D. Goetz and E. Neuscamman, “Suppressing Ionic Terms with Number-Counting Jastrow Factors in Real Space,” J. Chem. Theory Comput. **13**, 2035–2042 (2017).

<sup>76</sup>B. Van Der Goetz, L. Otis, and E. Neuscamman, “Clean and convenient tessellations for number counting jastrow factors,” J. Chem. Theory Comput. **15**, 1102–1121 (2019), <https://doi.org/10.1021/acs.jctc.8b01139>.

<sup>77</sup>F. Cordova, L. J. Dorio, A. Ipatov, M. E. Casida, C. Filippi, and A. Vela, “Troubleshooting time-dependent density-functional theory for photochemical applications: Oxirane,” J. Chem. Phys. **127**, 164111 (2007).

<sup>78</sup>C. Filippi, M. Zaccheddu, and F. Buda, “Absorption spectrum of the green fluorescent protein chromophore: A difficult case for ab initio methods?” J. Chem. Theory Comput. **5**, 2074–2087 (2009).

<sup>79</sup>R. Send, O. Valsson, and C. Filippi, “Electronic excitations of simple cyanine dyes: Reconciling density functional and wave function methods,” Journal of Chemical Theory and Computation **7**, 444–455 (2011), pMID: 26596164, <https://doi.org/10.1021/ct1006295>.

<sup>80</sup>R. Guareschi and C. Filippi, “Ground- and excited-state geometry optimization of small organic molecules with quantum monte carlo,” Journal of Chemical Theory and Computation **9**, 5513–5525 (2013), pMID: 26592286, <https://doi.org/10.1021/ct400876y>.

<sup>81</sup>R. Guareschi, H. Zulfikri, C. Daday, F. M. Floris, C. Amovilli, B. Mennucci, and C. Filippi, “Introducing qmc/mmmpol: Quantum monte carlo in polarizable force fields for excited states,” J. Chem. Theory Comput. **12**, 1674–1683 (2016).

<sup>82</sup>A. Cuzzocrea, A. Scemama, W. J. Briels, S. Moroni, and C. Filippi, “Variational principles in quantum monte carlo: The troubled story of variance minimization,” J. Chem. Theory Comput. **16**, 4203–4212 (2020), pMID: 32419451, <https://doi.org/10.1021/acs.jctc.0c00147>.

<sup>83</sup>L. Zhao and E. Neuscamman, “An Efficient Variational Principle for the Direct Optimization of Excited States,” J. Chem. Theory Comput. **12**, 3436–3440 (2016).

<sup>84</sup>J. A. R. Shea and E. Neuscamman, “Size consistent excited states via algorithmic transformations between variational principles,” J. Chem. Theory Comput. **13**, 6078–6088 (2017), pMID: 29140699, <https://doi.org/10.1021/acs.jctc.7b00923>.

<sup>85</sup>C. Filippi, R. Assaraf, and S. Moroni, “Simple formalism for efficient derivatives and multi-determinant expansions in quantum Monte Carlo,” J. Chem. Phys. **144**, 194105 (2016), [arXiv:1602.05490](https://doi.org/10.1063/1.4942590).

<sup>86</sup>R. Assaraf, S. Moroni, and C. Filippi, “Optimizing the Energy with Quantum Monte Carlo: A Lower Numerical Scaling for Jastrow–Slater Expansions,” J. Chem. Theory Comput. **13**, 5273–5281 (2017), [arXiv:1706.07588](https://doi.org/10.1021/acs.jctc.7b00923).

<sup>87</sup>S. D. Flores and E. Neuscamman, “Excited State Specific Multi-Slater Jastrow Wave Functions,” J. Phys. Chem. A **123**, 1487–1497 (2019), [arXiv:1811.00583](https://doi.org/10.1021/acs.jpca.8b08583).

<sup>88</sup>S. M. Garner and E. Neuscamman, “A variational monte carlo approach for core excitations,” The Journal of Chemical Physics **153**, 144108 (2020), <https://doi.org/10.1063/5.0020310>.

<sup>89</sup>L. N. Tran and E. Neuscamman, “Improving excited-state potential energy surfaces via optimal orbital shapes,” J. Phys. Chem. A **124**, 8273–8279 (2020).

<sup>90</sup>R. Hanscam and E. Neuscamman, “Applying generalized variational principles to excited-state-specific complete active space self-consistent field theory,” arXiv **2111.02590** (2021).

<sup>91</sup>P. J. Robinson, S. D. Pineda Flores, and E. Neuscamman, “Excitation variance matching with limited configuration interaction expansions in variational monte carlo,” J. Chem. Phys. **147**, 164114 (2017).

<sup>92</sup>L. Otis, I. Craig, and E. Neuscamman, “A hybrid approach to excited-state-specific variational monte carlo and doubly excited states,” The Journal of Chemical Physics **153**, 234105 (2020), <https://doi.org/10.1063/5.0024572>.

<sup>93</sup>B. M. Austin, D. Y. Zubarev, and W. A. Lester, “Quantum monte carlo and related approaches,” Chemical Reviews **112**, 263–288 (2012), <https://doi.org/10.1021/cr2001564>.

<sup>94</sup>W. M. C. Foulkes, L. Mitas, R. J. Needs, and G. Rajagopal, “Quantum Monte Carlo simulations of solids,” Rev. Mod. Phys. **73**, 33–83 (2001).

<sup>95</sup>C. J. Umrigar, J. Toulouse, C. Filippi, S. Sorella, and R. G. Hennig, “Alleviation of the fermion-sign problem by optimization of many-body wave functions,” Phys. Rev. Lett. **98**, 110201 (2007), 0611094 [cond-mat].

<sup>96</sup>S. Sorella, M. Casula, and D. Rocca, “Weak binding between two aromatic rings: Feeling the van der Waals attraction by quantum Monte Carlo methods,” J. Chem. Phys. **127**, 014105 (2007), [arXiv:0702349](https://doi.org/10.1063/1.27349) [cond-mat].

<sup>97</sup>E. Neuscamman, C. J. Umrigar, and G. K. L. Chan, “Optimizing large parameter sets in variational quantum Monte Carlo,” Phys. Rev. B **85**, 045103 (2012), [arXiv:1108.0900](https://doi.org/10.1103/1108.0900).

<sup>98</sup>L. Zhao and E. Neuscamman, “A Blocked Linear Method for Optimizing Large Parameter Sets in Variational Monte Carlo,” J. Chem. Theory Comput. **13**, 2604–2611 (2017).

<sup>99</sup>L. R. Schwarz, A. Alavi, and G. H. Booth, “Projector Quantum Monte Carlo Method for Nonlinear Wave Functions,” Phys. Rev. Lett. **118**, 176403 (2017), [arXiv:1610.09326](https://doi.org/10.1103/1610.09326).

<sup>100</sup>I. Sabzevari and S. Sharma, “Improved Speed and Scaling in Orbital Space Variational Monte,” J. Chem. Theory Comput. **14** (2018), 10.1021/acs.jctc.8b00780.

<sup>101</sup>L. Otis and E. Neuscamman, “Complementary first and second derivative methods for ansatz optimization in variational monte carlo,” Phys. Chem. Chem. Phys. **21**, 14491–14510 (2019).

<sup>102</sup>R. Assaraf and M. Caffarel, “Zero-variance principle for monte carlo algorithms,” Phys. Rev. Lett. **83**, 4682–4685 (1999).

<sup>103</sup>S. Pathak and L. K. Wagner, “A light weight regularization for wave function parameter gradients in quantum monte carlo,” AIP Advances **10**, 085213 (2020), <https://doi.org/10.1063/5.0004008>.

<sup>104</sup>J. van Rhijn, C. Filippi, S. D. Palo, and S. Moroni, “Energy derivatives in real-space diffusion monte carlo,” (2021), [arXiv:2105.09218](https://doi.org/10.1103/2105.09218) [cond-mat.mtrl-sci].

<sup>105</sup>R. Assaraf and M. Caffarel, “Computing forces with quantum monte carlo,” The Journal of Chemical Physics **113**, 4028–4034 (2000), <https://doi.org/10.1063/1.1286598>.

<sup>106</sup>R. Assaraf and M. Caffarel, “Zero-variance zero-bias principle for observables in quantum monte carlo: Application to forces,” The Journal of Chemical Physics **119**, 10536–10552 (2003), <https://doi.org/10.1063/1.1621615>.

<sup>107</sup>C. Attaccalite and S. Sorella, “Stable liquid hydrogen at high pressure by a novel ab initio molecular-dynamics calculation,” Phys. Rev. Lett. **100**, 114501 (2008).

<sup>108</sup>J. R. Trail, “Heavy-tailed random error in quantum monte carlo,” Phys. Rev. E **77**, 016703 (2008).

<sup>109</sup>J. R. Trail, “Alternative sampling for variational quantum monte carlo,” Phys. Rev. E **77**, 016704 (2008).

<sup>110</sup>M. P. Nightingale and V. Melik-Alaverdian, “Optimization of ground- and excited-state wave functions and van der waals clusters,” Phys. Rev. Lett. **87**, 43401 (2001).

<sup>111</sup>J. Toulouse and C. J. Umrigar, “Optimization of quantum monte carlo wave functions by energy minimization,” The Journal of Chemical Physics **126**, 084102 (2007), <https://doi.org/10.1063/1.2437215>.

<sup>112</sup>J. Toulouse and C. J. Umrigar, “Full optimization of jastrow–slater wave functions with application to the first-row atoms and homonuclear diatomic molecules,” The Journal of Chemical Physics **128**, 174101 (2008), <https://doi.org/10.1063/1.2908237>.

<sup>113</sup>D. Luo and B. K. Clark, “Backflow transformations via neural networks for quantum many-body wave functions,” Phys. Rev. Lett. **122**, 226401 (2019).

<sup>114</sup>A. Mahajan and S. Sharma, “Symmetry-projected jastrow mean-field wave function in variational monte carlo,” J. Phys. Chem. A **123**, 3911–3921 (2019), <https://doi.org/10.1021/acs.jpca.9b01583>.

<sup>115</sup>K. Nakano, C. Attaccalite, M. Barborini, L. Capriotti, M. Casula, E. Coccia, M. Dagrada, C. Genovese, Y. Luo, G. Mazzola, A. Zen, and S. Sorella, “Turborvb: A many-body toolkit for ab initio electronic simulations by quantum monte carlo,” The Journal of Chemical Physics **152**, 204121 (2020), <https://doi.org/10.1063/5.0005037>.

<sup>116</sup>A. A. Holmes, N. M. Tubman, and C. J. Umrigar, “Heat-Bath Configuration Interaction: An Efficient Selected Configuration Interaction Algorithm Inspired by Heat-Bath Sampling,” J. Chem. Theory Comput. **12**, 3674–3680 (2016), 1606.07453.

<sup>117</sup>S. Sharma, A. A. Holmes, G. Jeanmairet, A. Alavi, and C. J. Umrigar, “Semistochastic Heat-Bath Configuration Interaction Method: Selected Configuration Interaction with Semistochastic Perturbation Theory,” J. Chem. Theory Comput. **13**, 1595–1604 (2017), [arXiv:1610.06660v2](https://doi.org/10.1021/acs.jctc.6b00602).

<sup>118</sup>J. Kim, A. Baczeski, T. D. Beaudet, A. Benali, M. C. Bennett, M. A.

Berrill, N. S. Blunt, E. J. L. Borda, M. Casula, D. M. Ceperley, B. K. Clark, R. C. C. Iii, K. T. Delaney, M. Dewing, K. P. Esler, H. Hao, O. Heinonen, P. R. C. Kent, J. T. Krogel, I. Kylanpaa, Y. W. Li, M. G. Lopez, Y. Luo, F. D. Malone, R. M. Martin, A. Mathuriya, J. Mcminis, C. A. Melton, L. Mitas, M. A. Morales, E. Neuscamman, W. D. Parker, S. D. P. Flores, N. A. Romero, B. M. Rubenstein, J. A. R. Shea, H. Shin, L. Shulenburger, A. Tillack, J. P. Townsend, N. M. Tubman, B. Van Der Goetz, J. E. Vincent, D. C. Yang, Y. Yang, S. Zhang, and L. Zhao, "QMCPACK : An open source ab initio Quantum Monte Carlo package for the electronic structure of atoms, molecules, and solids," *J. Phys. Condens. Matter* **30**, 195901 (2018).

<sup>119</sup>P. R. C. Kent, A. Annaberdiyev, A. Benali, M. C. Bennett, E. J. Landinez Borda, P. Doak, H. Hao, K. D. Jordan, J. T. Krogel, I. Kylänpää, J. Lee, Y. Luo, F. D. Malone, C. A. Melton, L. Mitas, M. A. Morales, E. Neuscamman, F. A. Reboreda, B. Rubenstein, K. Saritas, S. Upadhyay, G. Wang, S. Zhang, and L. Zhao, "Qmcpack: Advances in the development, efficiency, and application of auxiliary field and real-space variational and diffusion quantum monte carlo," *J. Chem. Phys.* **152**, 174105 (2020), <https://doi.org/10.1063/5.0004860>.

<sup>120</sup>M. C. Bennett, C. A. Melton, A. Annaberdiyev, G. Wang, L. Shulenburger, and L. Mitas, "A new generation of effective core potentials for correlated calculations," *J. Chem. Phys.* **147**, 224106 (2017), <https://doi.org/10.1063/1.4995643>.

<sup>121</sup>Q. Sun, T. C. Berkelbach, N. S. Blunt, G. H. Booth, S. Guo, Z. Li, J. Liu, J. D. McClain, E. R. Sayfutyarova, S. Sharma, S. Wouters, and G. K.-L. Chan, "Pyscf: the python-based simulations of chemistry framework," *WIREs Computational Molecular Science* **8**, e1340 (2018), <https://onlinelibrary.wiley.com/doi/pdf/10.1002/wcms.1340>.

<sup>122</sup>H.-J. Werner, P. J. Knowles, G. Knizia, F. R. Manby, M. Schütz, *et al.*, "Molpro, version 2019.1, a package of ab initio programs," (2019), see <http://www.molpro.net>.

<sup>123</sup>G. M. J. Barca, C. Bertoni, L. Carrington, D. Datta, N. De Silva, J. E. Deustua, D. G. Fedorov, J. R. Gour, A. O. Gunina, E. Guidez, T. Harville, S. Irle, J. Ivanic, K. Kowalski, S. S. Leang, H. Li, W. Li, J. J. Lutz, I. Magoulas, J. Mato, V. Mironov, H. Nakata, B. Q. Pham, P. Piecuch, D. Poole, S. R. Pruitt, A. P. Rendell, L. B. Roskop, K. Ruedenberg, T. Sat-sathuchana, M. W. Schmidt, J. Shen, L. Slipchenko, M. Sosonkina, V. Sundriyal, A. Tiwari, J. L. Galvez Vallejo, B. Westheimer, M. Wloch, P. Xu, F. Zahariev, and M. S. Gordon, "Recent developments in the general atomic and molecular electronic structure system," *The Journal of Chemical Physics* **152**, 154102 (2020), <https://doi.org/10.1063/5.0005188>.

<sup>124</sup>R. R. Lucchese and H. F. Schaefer, "Charge-transfer complexes. ammonia-molecular fluorine, ammonia-molecular chlorine, ammonia-chlorine fluoride, trimethylamine-molecular fluorine, trimethylamine-molecular chlorine, and trimethylamine-chlorine fluoride," *Journal of the American Chemical Society* **97**, 7205–7210 (1975), <https://doi.org/10.1021/ja00858a001>.

<sup>125</sup>Y. Zhao and D. G. Truhlar, "Density functional for spectroscopy: No long-range self-interaction error, good performance for rydberg and charge-transfer states, and better performance on average than b3lyp for ground states," *The Journal of Physical Chemistry A* **110**, 13126–13130 (2006), pMID: 17149824, <https://doi.org/10.1021/jp066479k>.

<sup>126</sup>P. Piecuch, J. A. Hansen, and A. O. Ajala, "Benchmarking the completely renormalised equation-of-motion coupled-cluster approaches for vertical excitation energies," *Molecular Physics* **113**, 3085–3127 (2015), <https://doi.org/10.1080/00268976.2015.1076901>.

<sup>127</sup>J. Lorentzon, M. P. Fuelscher, and B. O. Roos, "Theoretical study of the electronic spectra of uracil and thymine," *Journal of the American Chemical Society* **117**, 9265–9273 (1995), <https://doi.org/10.1021/ja00141a019>.

<sup>128</sup>D. Kánnár and P. G. Szalay, "Benchmarking coupled cluster methods on singlet excited states of nucleobases," *Journal of Molecular Modeling* **20**, 2503 (2014).

<sup>129</sup>Y. Tawada, T. Tsuneda, S. Yanagisawa, T. Yanai, and K. Hirao, "A long-range-corrected time-dependent density functional theory," *The Journal of Chemical Physics* **120**, 8425–8433 (2004), <https://doi.org/10.1063/1.1688752>.

<sup>130</sup>N. S. Blunt and E. Neuscamman, "Charge-transfer excited states: Seeking a balanced and efficient wave function ansatz in variational monte carlo," *The Journal of Chemical Physics* **147**, 194101 (2017), <https://doi.org/10.1063/1.4998197>.

<sup>131</sup>D. Mester, P. R. Nagy, and M. Kállay, "Reduced-cost linear-response cc2 method based on natural orbitals and natural auxiliary functions," *The Journal of Chemical Physics* **146**, 194102 (2017), <https://doi.org/10.1063/1.4983277>.

<sup>132</sup>X. Feng, A. D. Becke, and E. R. Johnson, "Communication: Becke's virial exciton model gives accurate charge-transfer excitation energies," *The Journal of Chemical Physics* **149**, 231101 (2018), <https://doi.org/10.1063/1.5078515>.

<sup>133</sup>K. Hirao, B. Chan, J.-W. Song, and H.-S. Bae, "Charge-transfer excitation energies expressed as orbital energies of kohn-sham density functional theory with long-range corrected functionals," *The Journal of Physical Chemistry A* **124**, 8079–8087 (2020), pMID: 32901484, <https://doi.org/10.1021/acs.jpca.0c05414>.

<sup>134</sup>H. Jiang and P. M. Zimmerman, "Charge transfer via spin flip configuration interaction: Benchmarks and application to singlet fission," *The Journal of Chemical Physics* **153**, 064109 (2020), <https://doi.org/10.1063/5.0018267>.

<sup>135</sup>D. A. Fedotov, A. C. Paul, P. Posocco, F. Santoro, M. Garavelli, H. Koch, S. Coriani, and R. Imrota, "Excited-state absorption of uracil in the gas phase: Mapping the main decay paths by different electronic structure methods," *Journal of Chemical Theory and Computation* **17**, 1638–1652 (2021), pMID: 33529532, <https://doi.org/10.1021/acs.jctc.0c01150>.

<sup>136</sup>M. Vérit, A. Scemama, M. Caffarel, F. Lippurini, M. Boggio-Pasqua, D. Jacquemin, and P.-F. Loos, "Questdb: A database of highly accurate excitation energies for the electronic structure community," *WIREs Computational Molecular Science* **11**, e1517 (2021), <https://wires.onlinelibrary.wiley.com/doi/pdf/10.1002/wcms.1517>.